

CANDU

Degradation of Fracture Toughness by Hydride Embrittlement in CANDU Pressure Tube

• • • •

150

CANDU

DHC (Delayed Hydride Cracking)

• , AR 100

, 200 ppm

CANDU Zr-2.5Nb

300°C

가

가

가

,

가

AR

Abstract

Unpredictable failures can occur due to the DHC (delayed hydride cracking) or the degradation of fracture toughness by hydride embrittlement in CANDU pressure tube which can result from the absorption of hydrogen or deuterium in the high temperature coolant. To investigate the hydride embrittlement of CANDU Zr-2.5Nb pressure tube, the transverse tensile test and the fracture toughness test were performed from room temperature to 300°C using three different specimens which have an AR (As Received), 100, and 200 ppm hydrogen. As the amount of absorbed hydrogen was increased, the transverse yield strength and the ultimate tensile strength were also increased. In addition, as the test temperature became higher they were decreased linearly. While, at room temperature, the hydrogen-absorbed specimens represented the embrittlement which resulted in sudden decreasing of fracture toughness, the fracture characteristics became ductile such as AR specimen at high temperatures.

1.

가 18 CANDU 1 Zr-2.5wt%Nb
 가 [1], matrix Delayed
 Hydride Cracking (DHC) (Hydride)
 [2]. 1,2,3,4
 CANDU
 [3,4],
 가 .
 , , ASTM
 AECL
 Curved Compact Tension (CCT) ASTM
 [5,6]. CCT ASTM
 , burst test
 Zr-2.5Nb CCT

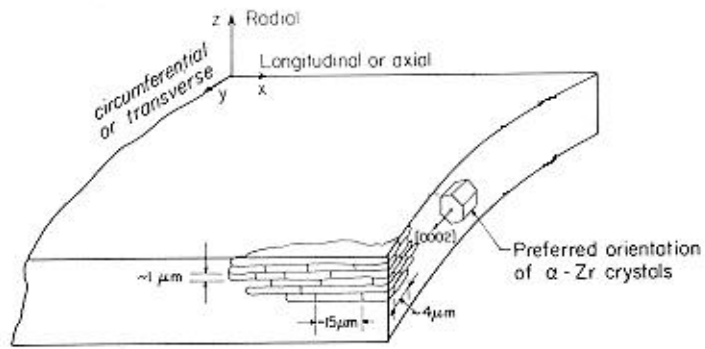
2.

2.1

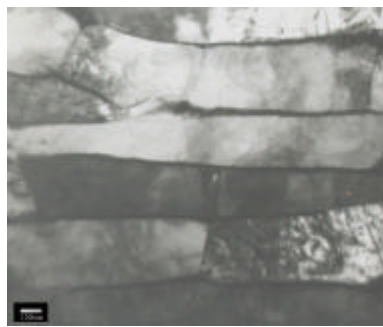
CANDU 4 cold-worked Zr-2.5Nb
 800°C 11:1 Hot Extrusion Cold Drawing (25%) 400 °C
 24 Autoclave . CANDU (11:1
) (Fig. 1).
 -Zr , -Zr -Zr -Zr (1)

Fig. 2

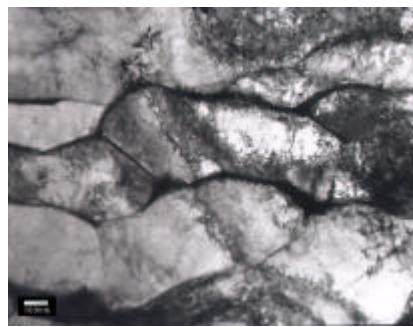
Zr-2.5Nb
 Axial-section a-Zr



(a) Zr-2.5Nb



(b) Axial Section



(c) Circumferential Section

Fig. 1 Typical Microstructure of Zr-2.5Nb Pressure Tube

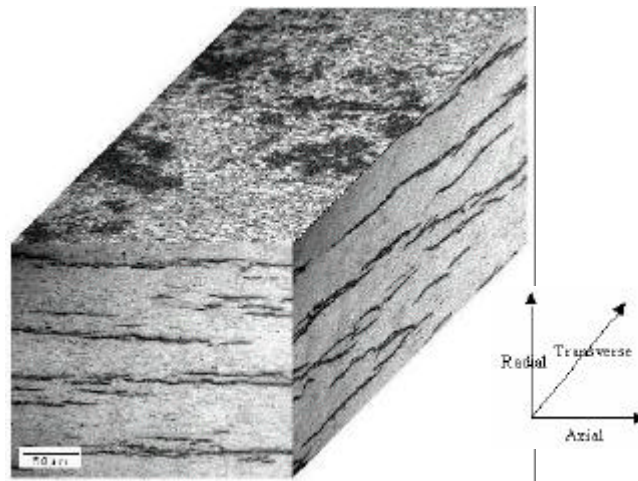


Fig. 2 Typical Microstructure of circumferential Hydride on Zr-2.5Nb Pressure Tube

Fig. 3(a)

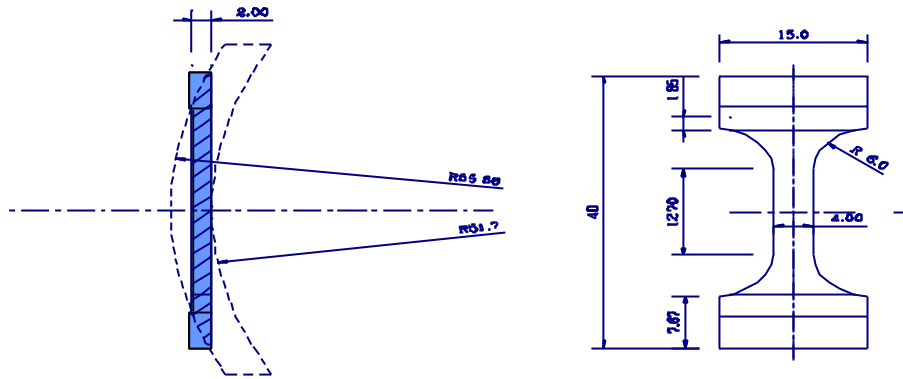
2 mm

Fig. 3(b) CANDU

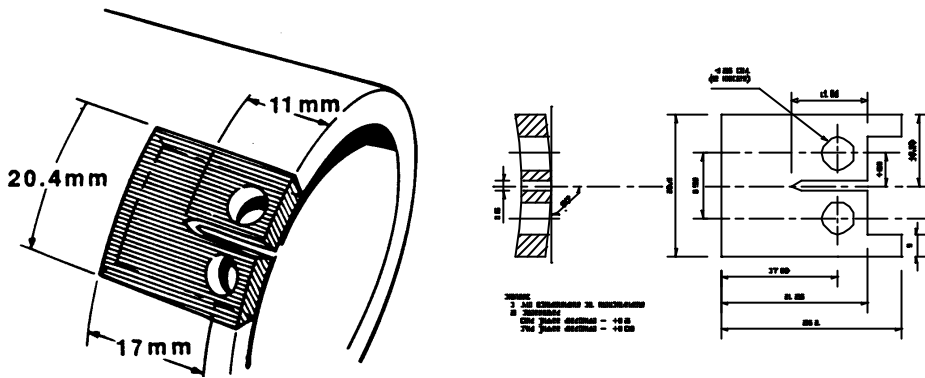
CCT

CCT

103 mm , 4.2~4.4 mm . CCT Axial
 , W 17 mm, (a_f/W) 0.4 .



(a) Transverse Tensile Specimen



(b) Collection and CCT Specimen

Fig. 3 Geometry of Transverse Tensile and CCT Specimen

2.2

2.2.1

Instron 8501 , Zr-2.5Nb 가
 , DCPD 800 °C 3
 . 0.5° ,
 [7]. ,
 DCPD , Nine point
 average method [8] DCPD .

2.2.2

(Cathodic Hydrogen Charging Method)

100, 200 ppm

KAERI

[9]

2

() $65\pm 5^\circ\text{C}$

0.1~0.2 molar

()

, 150

mA/cm^2

120

가 ,

50%

100 ppm

336°C

16.3 , 200 ppm

402°C

6.9

Hot

Vacuum Extraction

2.2.3

ASTM E 8 [10], 250°C

300°C

ASTM E 21 [11]

Instron

Series IX

, 0.2%

UTS

2.2.4

ASTM E 1737-96 [12]

single-specimen method

300°C

0.2 KN 가

가

1

soaking time

$\pm 3^\circ\text{C}$

, potential drop

Instron Fast Track JIC

300°C

10 heat-tinting

가

, 0.7

9-point average method

J-R

ASTM E-1152 [13] J

3.

3.1

Fig. 4 3 가

AR (As Received) , 100, 200 ppm

0.2% UTS 1 250, 300°C

ppm 가 , 200 ppm, AR

100

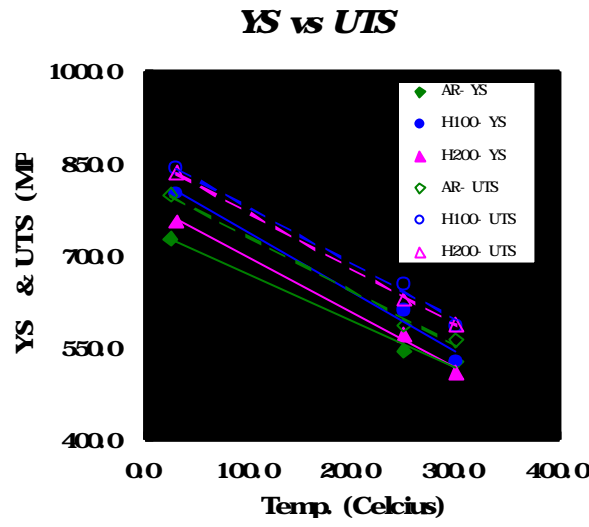


Fig. 4 YS and UTS of Transverse Tensile Test

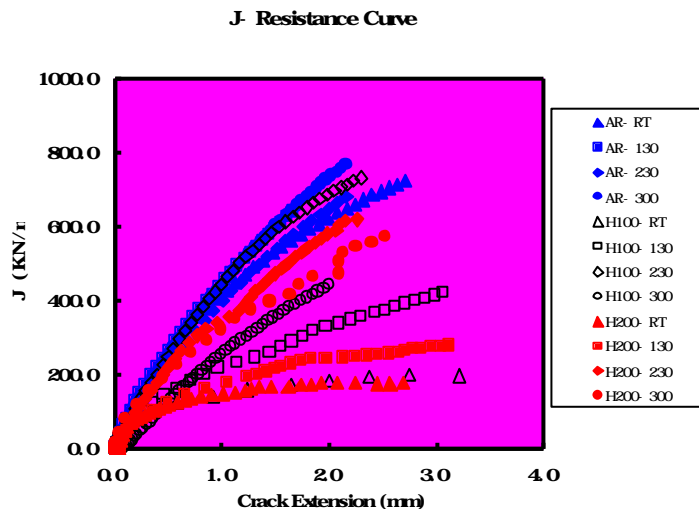


Fig. 5 J-R Curve Variation with the Temperatures

3.2 CCT

$J-R$, dJ/da , tearing modulus, $J(1.5 \text{ mm})$

Fig. 5 Zr-2.5Nb . CCT J-R . 3

가 (AR, H100, H200) . AR

가

230°C (◆) 가 , AR

(△) 가 , 130°C

(□) 가 가

300°C(O) 130°C 200 ppm 100 ppm

230°C 가 가 가 가 가

dJ/da Comparison

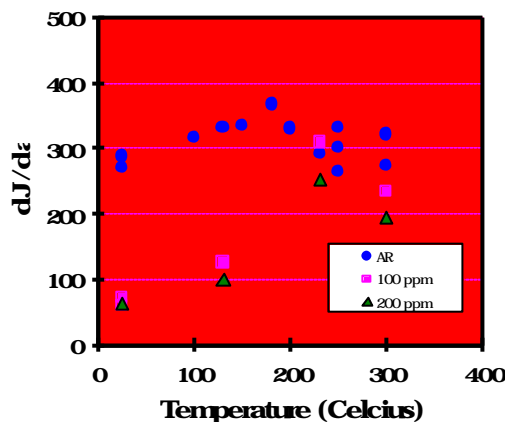


Fig. 6(a) dJ/da Variation with Temperature

Tearing Modulus

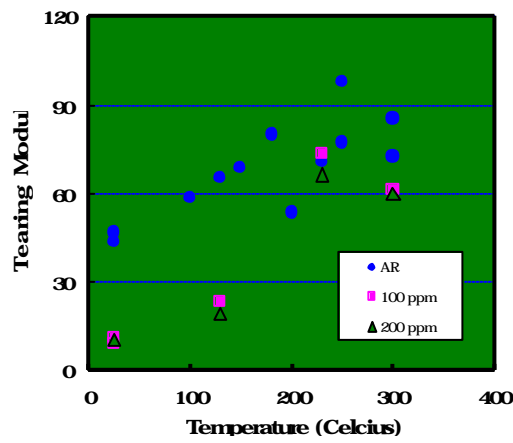


Fig. 6(b) Tearing Modulus Variation with Temperature

J(1.5 mm) Comparison

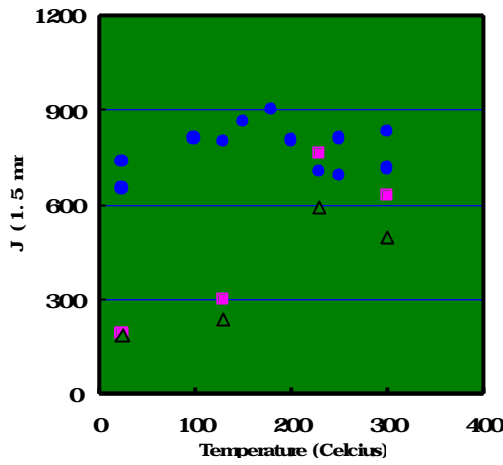


Fig. 6(c) $J(1.5 \text{ mm})$ Variation with Temperature

tearing modulus $J(1.5 \text{ mm})$. Fig. 6 (a)~(c) dJ/da 0.15 mm 1.5 mm

offset-line $J-R$, (tearing modulus) $T = \frac{E}{s_f^2} \frac{dJ}{da}$

J . $J(1.5 \text{ mm})$ 1.5 mm offset-line $J-R$

Fig. 6(a) dJ/da . AR (o) dJ/da

가 가 가 , 180°C 가 가

가

AR 가 230°C AR

가 300°C .

가

AR

Fig. 6(b) tearing modulus 가 가

Paris [14] dJ/da , flow

stress tearing modulus 가 가

Zr-2.5Nb T

가

Fig. 6(c) $J(1.5 \text{ mm})$,

dJ/da T .

4.

- AR 100, 200 ppm CANDU Zr-2.5Nb
300°C
- (1) Zr-2.5Nb 가 ,
300°C 가 .
- (2)
, 가 AR .
- (3) AR 가 (dJ/da , Tearing Modulus, $J_{1.5}$)

- [1] IAEA, IAEA-TECDOC-684, IAEA, Vienna, 1993, pp.7-56.
- [2] B.A. Cheadle et als, ASTM STP 939, ASTM, Philadelphia, 1987, pp.224-240.
- [3] A National Standard of Canada, CAN/CSA-N285.4-M94 (1994).
- [4] , " 1 (1994), 1994
- [5] L.A. Simpson, C.K. Chow, and P.H. Davies, "Standard Test Method for Fracture Toughness of CANDU Pressure Tubes", AECL Report COG-89-110-I, September 1989
- [6] D.D. Himbeault and P.H. Davies, "Second International Round Robin on Fracture Toughness Testing of Pressure Tube Materials Using 17 mm Curved Compact (Toughness) Specimens," RC-2069, COG-98-161-I, Jan. 1999, AECL
- [7] 4 , " Cold-worked Zr-2.5Nb CCL , " 2000 2 , pp. 239-244, 2000
- [8] British Standard Institute BS5447: 1977, "Plain Strain Fracture Toughness (K_{IC}) of Metallic Materials"
- [9] KAERI, "Zr-2.5Nb , " KAERI/TR-1329/99
- [10] American Society for Testing and Materials, ASTM E 8, "Standard Test Method of Tension Testing of Metallic Materials,"
- [11] American Society for Testing and Materials, ASTM E 8, "Standard Recommended Practice for Elevated Temperature Tension Tests of Metallic Materials"
- [12] American Society for Testing and Materials, ASTM E 1737-96, "Standard Test Method for J-Integral Characterization of Fracture Toughness"
- [13] American Society for Testing and Materials, ASTM E 1152-87, "Standard Test Method for Determining J-R Curves"
- [14] P.C. Paris et al, "The Theory of Instability of the Tearing Mode of Elastic Plastic Crack Growth," Elastic-Plastic Fracture, ASTM STP 668, American Society for Testing and Materials, pp. 5-36, (1979)